
[View Journal Online](#)
[View Article Online](#)

Structural and spectroscopic characterization and DFT studies of 2-amino-1,10-phenanthroline-1-ium chloride

 Sebile Işık Büyükeksi ^{1,*}, Namık Özdemir ² and Abdurrahman Şengül ¹
¹ Department of Chemistry, Faculty of Arts and Sciences, Zonguldak Bülent Ecevit University, Zonguldak, 67100, Turkey
 sebile.isik@gmail.com (S.I.B.), sengul@beun.edu.tr (A.Ş.)

² Department of Mathematics and Science Education, Faculty of Education, Ondokuz Mayıs University, Samsun, 55220, Turkey
 namiko@omu.edu.tr (N.Ö.)

 * Corresponding author at: Department of Chemistry, Faculty of Arts and Sciences, Zonguldak Bülent Ecevit University, Zonguldak, 67100, Turkey.
 Tel: +90.372.2911126 Fax: +90.372.2574181 e-mail: sebile.isik@gmail.com (S.I. Büyükeksi).

RESEARCH ARTICLE



doi: 10.5155/eurjchem.10.2.95-101.1847

Received: 11 March 2019

Received in revised form: 22 April 2019

Accepted: 04 May 2019

Published online: 30 June 2019

Printed: 30 June 2019

KEYWORDS

 Salt
 Spectroscopy
 DFT calculation
 X-ray structure
 Hydrogen bonding
 1,10-Phenanthroline

ABSTRACT

A versatile synthetic building block, 2-amino-1,10-phenanthroline-1-ium chloride (L-HCl) was synthesized and characterized by IR, ¹H and ¹³C NMR DEPT analysis, UV/Vis and single-crystal X-ray diffraction technique. The molecular geometry, vibrational wavenumbers and gauge including atomic orbital (GIAO), ¹H and ¹³C NMR chemical shifts values of the title compound in the ground state were obtained by using density functional theory (DFT/B3LYP) method with 6-311++G(d,p) basis set and compared with the experimental data. Electronic absorption spectrum of the salt was determined using the time-dependent density functional theory (TD-DFT) method at the same level. In the NMR and electronic absorption spectra calculations, the effect of solvent on the theoretical parameters was included using the default model with DMSO as solvent. The obtained theoretical parameters agree well with the experimental findings.

 Cite this: *Eur. J. Chem.* 2019, 10(2), 95-101

 Journal website: www.eurjchem.com

1. Introduction

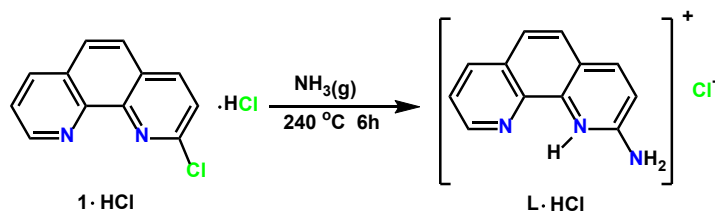
Among the molecular building blocks, charged species play an important role in molecular association processes in chemistry and biology [1,2]. Nevertheless, hydrogen bonding represents a very special class of chemical interactions that may bring about significant changes in the molecular and spectroscopic properties [3-5]. In particular, in order to observe or verify the changes in spectroscopic properties, the substituents or groups should directly involve in hydrogen bonding [6,7]. Hydrogen bonding interaction can be readily confirmed by FT-IR as observing the displacement of the frequency signals associated with stretches of the groups take part in hydrogen bonding [3]. NMR spectroscopy is another very useful technique that unambiguously shows the changes in chemical shift of the hydrogen nuclei forming the hydrogen bond [8]. Moreover, X-ray crystallography can be used to characterize the hydrogen bonded structure by determining the bond lengths of this type of interaction [9].

We have an ongoing interest in the synthesis of aza-bridged bis-1,10-phenanthroline derivatives [10-12], mainly due to their significant biological activity of the corresponding metal complexes in which the planar and also rigid structure

of 1,10-phenanthroline (phen) can either intercalate or bind to the grooves of DNA or RNA [13-20]. Therefore, the design and synthesis of new derivatives of phen with extended properties have gained a significant attention by many researchers [21-36]. We have previously reported an alternative strategy to synthesize a series of phen derivatives [37]. Recently, the site-selective alkylation of the acyclic aza-bridged bis-1,10-phenanthroline was reported by Kao *et al.* [10].

In recent years, many molecular properties, such as geometry, vibrational frequency etc. with high degree of accuracy in comparison to those of experimental values can be readily calculated by density functional theory methods [38-41].

To the best of our knowledge, neither the crystal structure and detailed spectroscopic investigation nor the theoretical studies on the title compound have been reported yet. The aim of this study is to investigate the structural and spectral properties of the compound in order to shed light on the reactivity of these intermediate using experimental and theoretical methods. Theoretical calculations have been carried out by using the density functional theory (B3LYP) method with B3LYP/6-311++G(d,p) basis set.



Scheme 1. Reaction conditions for the formation of 2-amino-1,10-phenanthroline-1-ium chloride.

2. Experimental

2.1. Materials and methods

We obtained all chemicals from commercial sources and used without further purification unless otherwise stated. Solvents were freshly distilled over appropriate drying reagents under dry N_2 atmosphere. The IR spectrum was recorded on a Perkin-Elmer Spectrum 100 FT-IR spectrophotometer with an attenuated total reflection (ATR) accessory featuring a zinc selenide (ZnSe) crystal. The 1H and ^{13}C NMR DEPT spectra have been measured in $DMSO-d_6$ with an Agilent 600 MHz Premium Compact NMR spectrometer at room temperature. Chemical shifts are given in parts per million with reference to TMS. The UV/Vis spectra have been measured on a PG Instruments T80+ UV-VIS spectrometer in DMSO.

2.2. Synthesis

The title salt (**L·HCl**) is mono-protonated as depicted in Scheme 1, because phen was previously obtained as a HCl salt to prevent sublimation in the tube where the reaction within the ammoniac gas carried out at 240 °C [10]. The final product has been purified by column chromatography (SiO_2 , dichloromethane:ethanol, 20:1, v:v) to afford a white precipitate. The single crystals suitable for X-ray diffraction analysis were grown by slow diffusion of dichloromethane into a concentrated ethanol solution. Color: White solid. Yield: 20%. IR (ATR, ν , cm^{-1}): 3459, 3295, 3179, 3039, 2923, 2852, 1622, 1589, 1553, 1510, 1491, 1462, 1418, 1394, 1366, 1294, 1229, 1142, 1083, 1029, 835, 770, 734, 660. 1H NMR (600 MHz, $DMSO-d_6$, δ , ppm): 8.9 (dd, 1H, $J = 8.92$ Hz, Ar-H), 8.3 (dd, 1H, $J = 8.31$ Hz, Ar-H), 8.02 (d, 1H, $J = 8.02$ Hz, Ar-H), 7.7 (d, 1H, $J = 7.70$ Hz, Ar-H), 7.6 (m, 1H, $J = 7.60$ Hz, Ar-H), 7.5 (d, 1H, $J = 7.54$ Hz, Ar-H), 6.9 (d, 1H, $J = 6.91$ Hz, Ar-H), 6.7 (s, 2H, NH_2). ^{13}C NMR (DEPT, 600 MHz, $DMSO-d_6$, δ , ppm): (C) 159.196, 145.594, 144.683, 129.257, 122.016, (CH) 148.966, 137.977, 136.192, 127.027, 122.805, 120.950, 112.644.

2.3. X-ray crystallography

Single-crystal X-ray diffraction data have been recorded with a Bruker APEX II QUAZAR three-circle diffractometer [42]. A total of 640 frames have been collected in the total exposure time of 10.67 h. The frames were integrated with the Bruker SAINT Software package using a wide-frame algorithm [43]. Data were corrected for absorption effects using the multi-scan method (SADABS) [44]. The structure was solved by a dual-space algorithm using SHELXT-2014 [45] and refined with full-matrix least-squares calculations on F^2 using SHELXL-2016 [46] implemented in WinGX [47] program suit. All H atoms were positioned geometrically and treated using a riding model, fixing the bond lengths at 0.86 and 0.93 Å for N-H and C-H, respectively. The displacement parameters of the H atoms were fixed at $U_{iso}(H) = 1.2U_{eq}$ of their parent atoms. Crystal structure validations and geometrical calculations were performed by using PLATON [48] software. Crystal data,

data collection and structure refinement details are summarized in Table 1.

2.4. Computational procedure

The DFT calculations with the three-parameter hybrid density functional (B3LYP) [49,50] and B3LYP/6-311++G(d,p) basis set [51] were performed using the Gaussian 03 software package [52] and GaussView visualization program [53]. The calculated vibrational frequencies ascertained that the structure was stable (no imaginary frequencies). Scale factors of 0.9679 (for wavenumbers under 1700 cm^{-1}) and 0.955 (for those over 1700 cm^{-1}) were used to correct the calculated harmonic vibrational frequencies [54]. The 1H and ^{13}C NMR chemical shifts were calculated within the gauge-independent atomic orbital (GIAO) approach [55,56], while the electronic absorption spectra were obtained using the time dependent density functional theory (TD-DFT) [57,58] at the same level. In these computations, solvent effects were included using the default method [59].

3. Results and discussion

3.1. Experimental and theoretical structures

An ORTEP-3 [47] view of which is shown in Figure 1. The compound crystallizes as a salt in the monoclinic space group $P2_1/n$ with $Z = 8$, and is composed of a singly protonated 2-amino-1,10-phenanthroline-1-ium cation and a chloride anion. There are two symmetry-independent molecules, labeled as A and B, in the asymmetric unit. In the following discussion, parameters for B are quoted in square brackets. Some of the optimized parameters (bond lengths, bond angles, and dihedral angles) of the compound using the B3LYP/6-311++G(d,p) method are listed in Table 2 together with the corresponding experimental data.

There is no chemically significant differences exist between the two cationic molecules in the asymmetric unit, as are evident from the root mean square (r.m.s.) bond and angle fit values of 0.006 Å and 0.549° obtained by PLATON (Figure 1 (b)). In addition, the two phen moieties inclined at an angle of 2.62(2)° are linked to each other by π - π stacking interactions, in which centroid-centroid separations change from 3.508(2) to 3.638(2) Å. As expected, the phen+ cation is planar, the r.m.s. deviation from the least-squares plane being 0.015(3) Å [0.052(3) Å], and the chloride ion which is hydrogen bonded to N1 and N2 deviates by only 0.149(2) Å [0.086(2) Å] from this plane. The N2-C1 and N2-C12 bond lengths of 1.343(4) and 1.381(4) Å [1.351(4) and 1.372(4) Å] for the protonated N2 atom are significantly longer than the corresponding lengths of 1.315(4) and 1.351(4) Å [1.312(4) and 1.358(4) Å] for the non-protonated N3 atom. These bond distances are calculated as 1.355, 1.369, 1.316 and 1.349 Å, respectively. Furthermore, the C1-N2-C12 angle of 123.0(3)° [123.0(3)°] at the protonated N2 atom is significantly larger than the corresponding angle of 116.4(3)° [116.7(3)°] at the non-protonated N3 atom. These angles are theoretically found to be 122.95 and 118.25°, respectively.

Table 1. Crystal data and structure refinement parameters for **L-HCl**.

| Parameters | L-HCl |
|---|---|
| CCDC deposition no. | 1507641 |
| Color/shape | Yellow/block |
| Chemical formula | (C ₁₂ H ₁₀ N ₃) ⁺ ·Cl ⁻ |
| Formula weight | 231.68 |
| Temperature (K) | 300(2) |
| Wavelength (Å) | 0.71073 MoKα |
| Crystal system | Monoclinic |
| Space group | P2 ₁ /n (No. 14) |
| Unit cell parameters | |
| <i>a</i> , <i>b</i> , <i>c</i> (Å) | 13.7908(5), 10.9756(4), 15.0251(5) |
| α , β , γ (°) | 90, 105.058(3), 90 |
| Volume (Å ³) | 2196.14(14) |
| <i>Z</i> | 8 |
| <i>D</i> _{calc} (g/cm ³) | 1.401 |
| μ (mm ⁻¹) | 0.321 |
| Absorption correction | Multi-scan |
| <i>T</i> _{min} , <i>T</i> _{max} | 0.61, 0.97 |
| <i>F</i> ₀₀₀ | 960 |
| Crystal size (mm ³) | 0.32 × 0.14 × 0.08 |
| Diffractometer | Bruker APEX II QUAZAR |
| Measurement method | φ and ω scans |
| Index ranges | -16 ≤ <i>h</i> ≤ 16, -13 ≤ <i>k</i> ≤ 7, -18 ≤ <i>l</i> ≤ 18 |
| θ range for data collection (°) | 1.787 ≤ θ ≤ 25.681 |
| Reflections collected | 17204 |
| Independent/observed reflections | 4173 / 2073 |
| <i>R</i> _{int} | 0.1033 |
| Refinement method | Full-matrix least-squares on <i>F</i> ² |
| Data/restraints/parameters | 4173/0/289 |
| Goodness-of-fit on <i>F</i> ² | 1.030 |
| Final <i>R</i> indices [<i>I</i> > 2 σ (<i>I</i>)] | <i>R</i> ₁ = 0.0577, <i>wR</i> ₂ = 0.1219 |
| <i>R</i> indices (all data) | <i>R</i> ₁ = 0.1386, <i>wR</i> ₂ = 0.1531 |
| $\Delta\rho_{\max}$, $\Delta\rho_{\min}$ (e/Å ³) | 0.29, -0.20 |

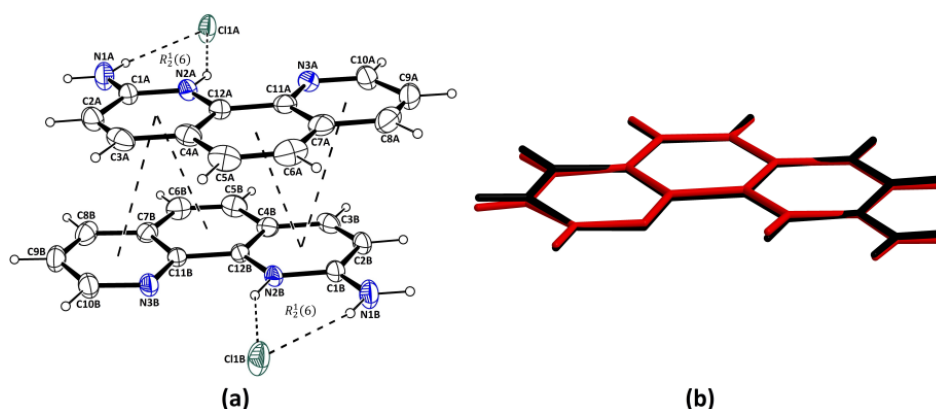


Figure 1. (a) The molecular structure of **L-HCl** showing the atom-labelling scheme. Displacement ellipsoids are drawn at the 30% probability level and H atoms are shown as small spheres of arbitrary radii. Intermolecular contacts are represented by broken lines. (b) A molecular fit of the two independent cationic molecules in the asymmetric unit (A = red, B = black).

These parameters are in the usual ranges, and comparable to those observed for similar structures reported in the literature [60-62].

When the experimental and computed structures are globally compared by overlaying them, the determined bond and angle fit values are 0.014 Å and 0.966° for A, and 0.013 Å and 0.676° for B (Figure 2). Consequently, the concordance between the theoretical and the x-ray structures is sufficient, and the computation level of theory can be used to reach the other properties.

Figure 3 shows the packing diagram obtained by Mercury 3.9 Software [63]. The compound contains no intramolecular hydrogen bond in the molecular structure. In the crystal structure, the cation is connected to the anion through N1-H...Cl1 and N2-H...Cl1 hydrogen bonds forming an $R_2^2(6)$ ring [64] (Figure 1). The cationic molecules are packed in π -stacked columns running along the *a* axis, the stacking sequence being AABBAABB. In this sequence, the centroid-centroid separations range from 3.508(2) to 3.767(2) Å. Even if these interactions are weak, they strongly contribute to the formation of a

stable 3D network [65]. The π -stacked columns are linked by N-H...Cl interactions, and have a tilting angle of 16.42° with respect to each other. The parameters for the hydrogen-bonding geometry are given in Table 3.

3.2. Spectroscopic characterization

The recorded and scaled theoretical spectra are given as superimposed in Figure 4. The vibrational bands assignments have been done by using Gauss View molecular visualization program. The amino group is generally considered as electron-donating substituent in aromatic ring system and the amino group involved in H-bonding leads to a reduction in the stretching wavenumber, an increase in the N-H₂ bending wavenumber, and an increase in infrared intensity. The observation of a broad band at 3459 cm⁻¹, at higher wavenumber compared that of 3320 cm⁻¹ observed for the non-protonated counterpart [21], assigned to N-H₂ stretching the primary amine having second band at lower wavenumber at 2852 cm⁻¹ is evident to H-bonding with chloride anion [66].

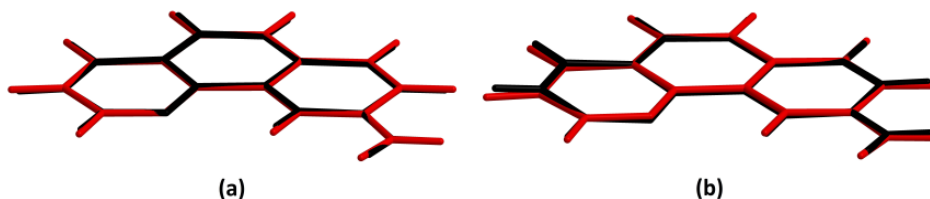
Table 2. Selected experimental and optimized geometric parameters for L-HCl.

| Parameters | X-Ray | | DFT |
|---------------------------|-----------|-----------|---------|
| | A | B | |
| Bond lengths (Å) | | | |
| N1-C1 | 1.320(4) | 1.318(4) | 1.327 |
| N2-C1 | 1.343(4) | 1.351(4) | 1.355 |
| N2-C12 | 1.381(4) | 1.372(4) | 1.369 |
| N3-C10 | 1.315(4) | 1.312(4) | 1.316 |
| N3-C11 | 1.351(4) | 1.358(4) | 1.349 |
| Bond angles (°) | | | |
| C1-N2-C12 | 123.0(3) | 123.0(3) | 122.95 |
| C10-N3-C11 | 116.4(3) | 116.7(3) | 118.25 |
| N1-C1-N2 | 119.7(3) | 119.4(3) | 118.48 |
| N1-C1-C2 | 121.8(3) | 122.7(3) | 123.31 |
| N2-C1-C2 | 118.4(3) | 117.9(3) | 118.21 |
| N2-C12-C11 | 118.5(3) | 118.9(3) | 119.54 |
| N2-C12-C4 | 119.5(3) | 119.8(3) | 120.30 |
| N3-C10-C9 | 124.8(4) | 124.2(3) | 123.21 |
| N3-C11-C7 | 124.1(3) | 123.7(3) | 123.49 |
| N3-C11-C12 | 118.5(3) | 118.0(3) | 117.83 |
| Torsion angles (°) | | | |
| N3-C11-C12-N2 | -0.6(5) | -179.7(3) | -0.01 |
| C12-N2-C1-N1 | -179.3(3) | 177.8(3) | 179.99 |
| N1-C1-C2-C3 | 179.7(4) | -179.3(3) | -179.99 |
| C5-C4-C12-N2 | 179.6(3) | -179.1(3) | -180.00 |
| C6-C7-C11-N3 | -179.2(3) | -179.3(3) | -179.99 |

Table 3. Hydrogen bonding geometry for L-HCl.

| D—H...A | D—H (Å) | H...A (Å) | D...A (Å) | D—H...A (°) |
|-------------------------------|---------|-----------|-----------|-------------|
| N1B-H1B2...C11B ⁱ | 0.86 | 2.36 | 3.182(3) | 159 |
| N1A-H1A2...C11A ⁱⁱ | 0.86 | 2.40 | 3.214(3) | 157 |
| N1B-H1B1...C11B | 0.86 | 2.33 | 3.133(3) | 156 |
| N1A-H1A1...C11A | 0.86 | 2.33 | 3.125(3) | 154 |
| N2A-H2A...C11A | 0.86 | 2.44 | 3.214(3) | 150 |
| N2B-H2B...C11B | 0.86 | 2.48 | 3.254(3) | 150 |

Symmetry codes: ⁱ -x+3/2, y-1/2, -z+3/2; ⁱⁱ -x+3/2, y+1/2, -z+1/2.

**Figure 2.** (a) A molecular fit of the calculated cationic structure (red) over molecule A (black). (b) A molecular fit of the calculated cationic structure (red) over molecule B (black).

These bands were calculated at 3503 and 2615 cm^{-1} , respectively. The secondary amine group was characterized by the N-H stretching vibration band at around 2923 cm^{-1} , which was observed at 2747 cm^{-1} in the theoretical spectra. Protonation causes this band to red shift with broadening of the band [67]. The slight deviations between the experimentally observed and the theoretically calculated amino group frequencies may be attributed to intermolecular hydrogen bond formation of the electron donating amino group. The hydrogen bonding facility of the amino group in the 1,10-phenanthroline ring system is of great interest in developing of supramolecular receptors for binding urea [26] and biological system for the recognition of a cytosine bulge and a cytosine-cytosine mismatch [29]. The cryptand-like receptors having ammonium groups are early known first type of hosts for binding halide anions [68,69]. We assigned the bands at 1510 cm^{-1} due to the N-H₂ scissoring which coincidence with theoretical value of 1565 cm^{-1} .

The C-H stretching frequency generally occurs in the wavenumber region 3100-3000 cm^{-1} [59]. The C-H aromatic stretching modes were observed in the range of 3295-3030 cm^{-1} experimentally and were calculated in the range of 3056-3017 cm^{-1} . The bands observed at 1394, 1366 and 1294 cm^{-1} have been assigned to C-H in-plane bending vibrations that were calculated at 1384, 1371 and 1294 cm^{-1} , respectively. The C-H out-of-plane deformation is provided between 1000

and 700 cm^{-1} . The C-H out-of-plane deformation mode recorded at 835 cm^{-1} is in good agreement with theoretical result of 826 cm^{-1} .

The aromatic ring C=C and C=N stretching vibrational modes appear in the region 1635-1100 and 1600-1500 cm^{-1} , respectively [67]. The ring C=C and C=N vibrations are coupled with other vibrations. They are not much affected by the substituents in the phen ring. The observed wavenumbers fall in the expected region of the spectrum [67]. The C=C and C=N stretching vibration modes were recorded at 1622 and 1589 cm^{-1} , and were appeared at 1645 and 1601 cm^{-1} , respectively, in the theoretical spectrum.

The structure of the title salt was clearly confirmed by ¹H and ¹³C NMR DEPT spectra. Due to presence of the amino group in the 2-position of phen, all the aromatic protons get resonance at different chemical shift. Thus, the eight aromatic protons are observed between δ 8.90 to 6.90 ppm. The chemical shifts are comparable to those observed for the free 2-amino-1,10-phenanthroline [29]. The protonation brought about slightly deshielding of the most protons in comparison to those of the non-protonated counterpart, but with the exception of the ortho-proton monitored at δ 8.90 ppm, whereas it appears at δ 9.09 ppm for the non-protonated counterpart. The amino group was clearly confirmed by the D₂O exchange experiment in which the signal corresponds to the NH₂ at δ 6.70 ppm was disappeared after deuteration.

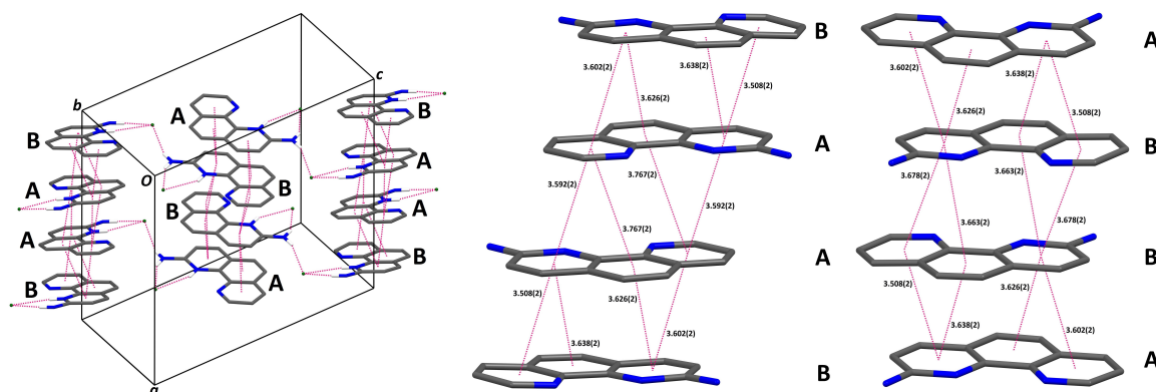


Figure 3. Packing diagram of **L·HCl**. Intermolecular N-H...Cl and π - π stacking interactions are shown as dashed lines and only H atoms involved in hydrogen bonding have been included. Distances are in Å.

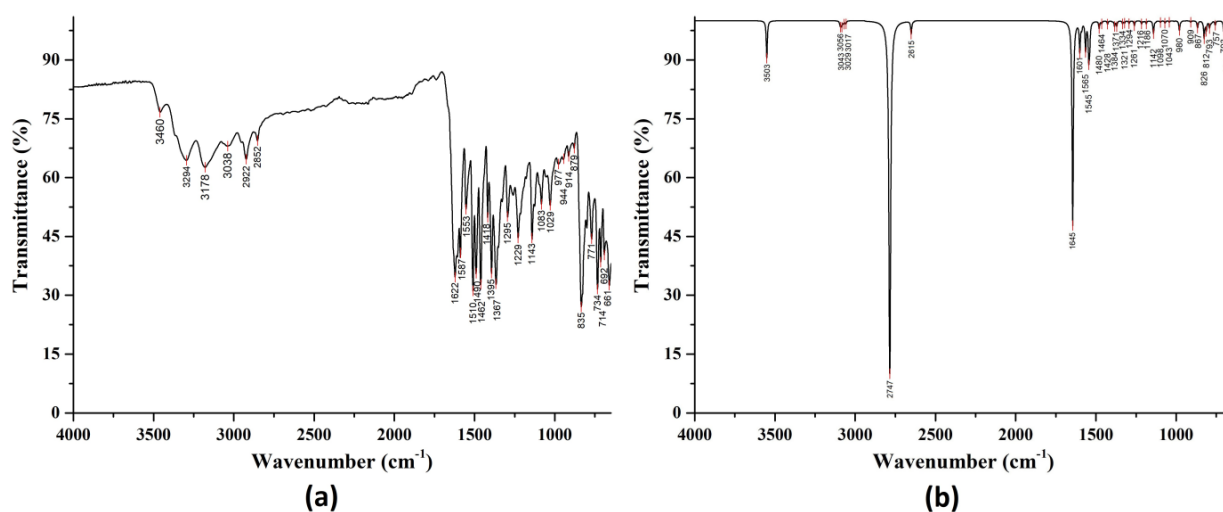


Figure 4. The experimentally recorded (a) and theoretically simulated (b) FT-IR spectra of **L·HCl**.

The structure was further characterized by ^{13}C NMR DEPT showing the five quaternary C atoms and seven CH atoms, respectively, in the expected range as compared to the free form [29].

The results of NMR calculations for the optimized structure are compared to those of experimental values in Table 4. The calculated ^1H chemical shift values of δ 7.14-16.07 ppm are different than those of the experimental values observed at δ 6.70-8.90 ppm. The aromatic protons observed at δ 6.90-8.90 ppm in the spectra, and were calculated at δ 7.14-9.40 ppm in the lower field. Additionally, the title compound gave distinctive singlet peak at δ 6.70 ppm experimentally, but calculated at δ 9.33 ppm. The calculated ^{13}C chemical shift values of δ 120.99-162.34 ppm are comparable to δ 112.60-160.30 ppm of the experimental values. The chemical shifts of almost all carbons in heterocyclic ring are set downfield, because of the presence of the protonated N atom of the phen ring. As can be seen from Table 4, the theoretical ^1H and ^{13}C chemical shift values are generally closer to the experimental data. The differences between the calculated and the experimental values can be explained by the fact that the classical hydrogen bonding (Table 3) causing polarization of the bonds, along with the protonation of the phen N atom as causing electron deficient at the certain position such as *ortho* and *para* positions, and also close stacking as an anti-parallel fashion where the amino groups can act as an electron donating group in dimer in addition to π - π interactions between the two planes. The solvent influence and also

polarity of the solvent should take into account for the differences as revealed in similar cases [70].

The electronic absorption spectrum of the title salt is shown in Figure 5. The band near at 330 nm is attributed to intra-ligand (IL) $\pi \rightarrow \pi^*$ transitions. The lowest energy bands at 330-450 nm are assigned to charge transfer (CT) transition due to protonation of the nitrogen atoms of the 1,10-phenanthroline moiety akin to those of heterocyclic compounds containing amines in which protonation leads to red shift [71]. It is also very well known that the lowest energy CT transitions are linearly related to the difference between the highest occupied molecular orbital (HOMO) and lowest unoccupied molecular orbital (LUMO). These bands in general show solvatochromic shift, as increasing polarity of the solvent the absorption maxima undergo red shift [72].

Electronic absorption spectrum of the title salt was computed by the TD-DFT method at the same level. To designate the major contributions of the transitions, GaussSum program [73] was used. According to the TD-DFT calculation, a single absorption was predicted at 346 nm with a major transition contribution from HOMO to LUMO (95%). The HOMO is localized on the chloride anion, while the LUMO is mainly spread over the phen cation and mostly the π -antibonding type orbitals (Figure 5). The HOMO-LUMO gap (ΔE) is an indicator of the chemical reactivity and chemical hardness-softness of a molecule, HOMO-LUMO gap becomes small for soft molecules and large for hard molecules. According to the calculated gap value of 2.98 eV, the title salt can be accepted as a soft molecule [74].

Table 4. Experimental and theoretical ^{13}C and ^1H NMR chemical shifts δ (ppm) from TMS for L·HCl.

| Atom ^a | Experimental | Calculated ^b | Atom ^a | Experimental | Calculated ^b |
|-------------------|--------------|-------------------------|-----------------------|--------------|-------------------------|
| C1 | 160.30 | 162.34 | C12 | 140.74 | 143.33 |
| C2 | 112.60 | 120.99 | H1 (NH ₂) | 6.70 | 9.33 |
| C3 | 150.73 | 150.90 | H2 (NH) | - | 16.07 |
| C4 | 120.90 | 126.98 | H2 | 6.90 | 7.14 |
| C5 | 131.35 | 132.92 | H3 | 8.00 | 8.49 |
| C6 | 127.00 | 131.11 | H5 | 7.60 | 8.09 |
| C7 | 135.77 | 137.69 | H6 | 7.70 | 8.15 |
| C8 | 142.56 | 144.24 | H8 | 8.30 | 8.66 |
| C9 | 122.80 | 131.58 | H9 | 7.50 | 8.01 |
| C10 | 155.48 | 156.82 | H10 | 8.90 | 9.40 |
| C11 | 143.36 | 144.95 | | | |

^aThe atom numbering according to Figure 1 (a) used in the assignment of chemical shifts.

^bAverage.

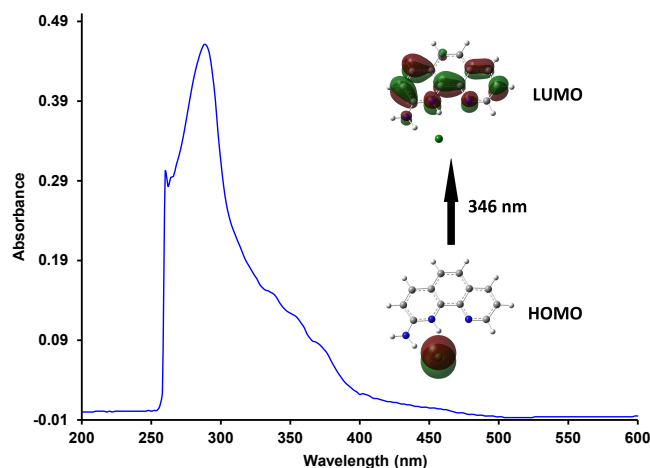


Figure 5. UV/Vis spectra of L·HCl in DMSO, and HOMO/LUMO orbital surfaces.

In the light of expressions given in the literature [75], the other calculated electronic parameters such as the ionization potential (I), electron affinity (A), chemical hardness (η), softness (S) and electronegativity (χ) are 5.69 eV, 2.71 eV, 1.49 eV, 0.34 eV⁻¹ and 4.2 eV, respectively.

4. Conclusion

In the present work, a new phenanthroline salt molecule has been synthesized and characterized by FT-IR, ^1H and ^{13}C NMR DEPT, UV/Vis and X-ray crystallography. X-ray results show that the π - π stacking interactions are mainly responsible for the stabilization of the crystal structure together with N-H...Cl interactions between the phen cation and chloride anion. The ^1H NMR and ^{13}C NMR spectra clearly confirm the molecular structure. The results of experimental studies are also supported by some quantum mechanics calculations at the B3LYP/6-311++G(d,p) level. TD-DFT calculations have been performed to determine possible electronic transitions. The calculated HOMO-LUMO gap energy is 2.98 eV, pointing to a soft molecule. Despite the little differences, there is found an acceptable correlation between the computational and the experimental results.

Acknowledgements

This work was supported by the Turkish Scientific and Technical Research Council (TÜBİTAK) [Grant number 214Z090].

Supporting information S

CCDC-1507641 contains the supplementary crystallographic data for this paper. These data can be obtained free of

charge via <https://www.ccdc.cam.ac.uk/structures/>, or by e-mailing data_request@ccdc.cam.ac.uk, or by contacting The Cambridge Crystallographic Data Centre, 12 Union Road, Cambridge CB2 1EZ, UK; fax: +44(0)1223-336033.

Disclosure statement DS

Conflict of interests: The authors declare that they have no conflict of interest.

Author contributions: All authors contributed equally to this work.

Ethical approval: All ethical guidelines have been adhered.

Sample availability: Samples of the compounds are available from the author.

ORCID ID

Sebile Işık Büyükekşi

<http://orcid.org/0000-0002-6075-1725>

Namık Özdemir

<http://orcid.org/0000-0003-3371-9874>

Abdurrahman Şengül

<http://orcid.org/0000-0001-6851-4612>

References

- Guerfel, T.; Bdiri, M.; Jouini, A. *J. Chem. Crystallogr.* **2000**, *30*(12), 799-804.
- Kanyo, Z. F.; Christianson, D. W. *J. Biol. Chem.* **1991**, *266*(7), 4264-4268.
- Belarmino, M. K.; Cruz, V. F.; Lima, N. B. *J. Mol. Model.* **2014**, *20*, 2477, 1-7.
- Hammami, F.; Ghalla, H.; Nasr, S. *Comput. Theor. Chem.* **2015**, *1070*, 40-47.
- Lima, N. B.; Ramos, M. N. *J. Mol. Struct.* **2012**, *1008*, 29-34.
- Abraham, R. J.; Mobli, M. *Magn. Reson. Chem.* **2007**, *45*(10), 865-877.

- [7]. Rusu, V. H.; da Silva, J. B. P.; Ramos, M. N. *Vib. Spectrosc.* **2008**, *46*(1), 52-56.
- [8]. Lomas, J. S. *Magn. Reson. Chem.* **2014**, *52*(12), 745-754.
- [9]. Shan, N.; Batchelor, E.; Jones, W. *Tetrahedron Lett.* **2002**, *43*(48), 8721-8725.
- [10]. Kao, H. C.; Hsu, C. J.; Hsu, C. W.; Lin, C. H.; Wang, W. J. *Tetrahedron Lett.* **2010**, *51*(29), 3743-3747.
- [11]. Chen, Z. J.; Wang, L. M.; Zou, G.; Zhang, L.; Zhang, G. J.; Cai, X. F.; Teng, M. S. *Dyes Pigments* **2012**, *94*(3), 410-415.
- [12]. Wang, W. J.; Sengul, A.; Luo, C. F.; Kao, H. C.; Cheng, Y. H. , *Tetrahedron Lett.* **2003**, *44*(37), 7099-7101.
- [13]. Cheng, C. C.; Kuo, Y. N.; Chuang, K. S.; Luo, C. F.; Wang, W. J. *Angew. Chem. Int. Ed.* **1999**, *38*(9), 1255-1257.
- [14]. Davis, J. T. *Angew. Chem. Int. Ed.* **2004**, *43*(6), 668-698.
- [15]. Hirai, M.; Shinozuka, K.; Sawai, H.; Ogawa, S. *Chem. Lett.* **1992**, *21*(10), 2023-2026.
- [16]. Reed, J. E.; Neidle, S.; Vilar, R. *Chem. Commun.* **2007**, *42*, 4366-4368.
- [17]. Tan, J. H.; Gu, L. Q.; Wu, J. Y. *Mini Rev. Med. Chem.* **2008**, *8*(11), 1163-1178.
- [18]. Yıldız, U.; Sengul, A.; Kandemir, I.; Comert, F.; Akkoc, S.; Coban, B. *Bioorg. Chem.* **2019**, *87*, 70-77.
- [19]. Polloni, L.; de Seni Silva, A. C.; Teixeira, S. C.; de Vasconcelos Azevedo, F. V. P.; Zoia, M. A. P.; da Silva, M. S.; Lima, P. M. A. P.; Correia, L. I. V.; do Couto Almeida, J.; da Silva, C. V. o, *Biomed. Pharmacother.* **2019**, *112*, 108586.
- [20]. Yu, B.; Rees, T. W.; Liang, J.; Jin, C.; Chen, Y.; Ji, L.; Chao, H. o, *Dalton Trans.* **2019**, *48*, 3914-3921.
- [21]. Akerboom, S.; van den Elshout, J. J.; Mutikainen, I.; Siegler, M. A.; Fu, W. T.; Bouwman, E. *Eur. J. Inorg. Chem.* **2013**, *36*, 6137-6146.
- [22]. Bezencon, J.; Wittwer, M. B.; Cutting, B.; Smiesko, M.; Wagner, B.; Kansy, M.; Ernst, B. *J. Pharm. Biomed. Anal.* **2014**, *93*, 147-155.
- [23]. Claus, K. G.; Rund, J. V. *Inorg. Chem.* **1969**, *8*(1), 59-63.
- [24]. Concepcion, J.; Just, O.; Leiva, A. M.; Loeb, B.; Rees, W. S. *Inorg. Chem.* **2002**, *41*(23), 5937-5939.
- [25]. Corey, E.; Borrer, A.; Foglia, T. J. *Org. Chem.* **1965**, *30*(1), 288-290.
- [26]. Engel, Y.; Dahan, A.; Rozenshine-Kemelmakher, E.; Gozin, M. *J. Org. Chem.* **2007**, *72*(7), 2318-2328.
- [27]. Krapcho, A. P.; Sparapani, S.; Leenstra, A.; Seitz, J. D. *Tetrahedron Lett.* **2009**, *50*(26), 3195-3197.
- [28]. Kumar, P.; Madyal, R. S.; Joshi, U.; Gaikar, V. G. *Ind. Eng. Chem. Res.* **2011**, *50*(13), 8195-8203.
- [29]. Li, J.; Matsumoto, J.; Otabe, T.; Dohno, C.; Nakatani, K. *Biorg. Med. Chem.* **2015**, *23*(4), 753-758.
- [30]. Maqsood, S. R.; Islam, N.; Bashir, S.; Khan, B.; Pandith, A. H. *J. Coord. Chem.* **2013**, *66*(13), 2308-2315.
- [31]. Hu, Z.; Miao, J.; Li, T.; Liu, M.; Murtaza, I.; Meng, H. *Nano Energy* **2018**, *43*, 72-80.
- [32]. Zhang, H. R.; Jin, X. X.; Zhou, X.; Zhang, Y.; Leung, C. F.; Xiang, J. *Cryst. Res. Technol.* **2019**, *54*(1), 1800168.
- [33]. Buyukeksi, S. I.; Karatay, A.; Acar, N.; Kucukoz, B.; Elmali, A.; Sengul, A. *Dalton Trans.* **2018**, *47*(22), 7422-7430.
- [34]. Buyukeksi, S. I.; Karatay, A.; Acar, N.; Kucukoz, B.; Elmali, A.; Sengul, A. *J. Photochem. Photobiol. A: Chem.* **2019**, *372*, 226-234.
- [35]. Buyukeksi, S. I.; Sengul, A.; Ergonmez, S.; Altindal, A.; Orman, E. B.; Ozkaya, A. R. *Dalton Trans.* **2018**, *47*(8), 2549-2560.
- [36]. Zwart, M.; Bastiaans, H.; Van der Goot, H.; Timmerman, H. *J. Med. Chem.* **1991**, *34*(3), 1193-1201.
- [37]. Wang, W. J.; Chuang, K. S.; Luo, C. F.; Liu, H. Y. *Tetrahedron Lett.* **2000**, *41*(44), 8565-8568.
- [38]. Firinci, R.; Gunay, M. E.; Ozdemir, N.; Dincer, M. *J. Mol. Struct.* **2017**, *1146*, 267-272.
- [39]. Issa, T. B.; Ghalla, H.; Marzougui, S.; Benhamada, L. *J. Mol. Struct.* **2017**, *1150*, 127-134.
- [40]. Ozdemir, N.; Kagit, R.; Dayan, O. *Mol. Phys.* **2016**, *114*(6), 757-768.
- [41]. Asath, R. M.; Rekha, T.; Premkumar, S.; Mathavan, T.; Benial, A. M. *F. J. Mol. Struct.* **2016**, *1125*, 633-642.
- [42]. Bruker, APEX II, Bruker, Bruker AXS Inc., Madison, Wisconsin, USA. 2014.
- [43]. Bruker, SAINT, Bruker, Bruker AXS Inc., Madison, Wisconsin, USA. 2013.
- [44]. Bruker, SADABS, Bruker, Bruker AXS Inc., Madison, Wisconsin, USA. 2014.
- [45]. Sheldrick, G. M. *Acta Crystallogr. Sect. A. Found. Adv.* **2015**, *71*(1), 3-8.
- [46]. Sheldrick, G. M. *Acta Crystallogr. Sect. C. Struct. Chem.* **2015**, *71*(1), 3-8.
- [47]. Farrugia, L. J. *J. Appl. Crystallogr.* **2012**, *45*(4), 849-854.
- [48]. Spek, A. L. *Acta Crystallogr. Sect. D* **2009**, *65*(2), 148-155.
- [49]. Becke, A. D. *J. Chem. Phys.* **1993**, *98*(7), 5648-5652.
- [50]. Lee, C.; Yang, W.; Parr, R. G. *Phys. rev. B* **1988**, *37*(2), 785-789.
- [51]. Ditchfield, R.; Hehre, W. J.; Pople, J. A. *J. Chem. Phys.* **1971**, *54*(2), 724-728.
- [52]. Frisch, M. J.; Trucks, G. W.; Schlegel, H. B.; Scuseria, G. E.; Robb, M. A.; Cheeseman, J. R.; Montgomery, Jr., J. A.; Vreven, T.; Kudin, K. N.; Burant, J. C.; Millam, J. M.; Iyengar, S. S.; Tomasi, J.; Barone, V.; Mennucci, B.; Cossi, M.; Scalmani, G.; Rega, N.; Petersson, G. A.; Nakatsuji, H.; Hada, M.; Ehara, M.; Toyota, K.; Fukuda, R.; Hasegawa, J.; Ishida, M.; Nakajima, T.; Honda, Y.; Kitao, O.; Nakai, H.; Klene, M.; Li, X.; Knox, J. E.; Hratchian, H. P.; Cross, J. B.; Bakken, V.; Adamo, C.; Jaramillo, J.; Gomperts, R.; Stratmann, R. E.; Yazyev, O.; Austin, A. J.; Cammi, R.; Pomelli, C.; Ochterski, J. W.; Ayala, P. Y.; Morokuma, K.; Voth, G. A.; Salvador, P.; Dannenberg, J. J.; Zakrzewski, V. G.; Dapprich, S.; Daniels, A. D.; Strain, M. C.; Farkas, O.; Malick, D. K.; Rabuck, A. D.; Raghavachari, K.; Foresman, J. B.; Ortiz, J. V.; Cui, Q.; Baboul, A. G.; Clifford, S.; Cioslowski, J.; Stefanov, B. B.; Liu, G.; Liashenko, A.; Piskorz, P.; Komaromi, I.; Martin, R. L.; Martin, R. L.; Keith, T.; Al-Laham, M. A.; Peng, C. Y.; Nanayakkara, A.; Challacombe, M.; Gill, P. M. W.; Johnson, B.; Chen, W.; Wong, M. W.; Gonzalez, C.; and Pople, J. A.; Gaussian, Inc., Wallingford CT, 2004. Frisch, M.; Trucks, G.; Schlegel, H.; Scuseria, G.; Robb, M.; Cheeseman, J.; Montgomery Jr, J.; Vreven, T.; Kudin, K.; Burant, J. Gaussian 03, Revision E. 01. 2004.
- [53]. Dennington, R.; Keith, T.; Millam, J. G. *Semichem Inc.* 2007.
- [54]. Andersson, M. P.; Uvdal, P. *J. Phys. Chem. A* **2005**, *109*(12), 2937-2941.
- [55]. Ditchfield, R. *J. Chem. Phys.* **1972**, *56*(11), 5688-5691.
- [56]. Wolinski, K.; Hinton, J. F.; Pulay, P. *J. Am. Chem. Soc.* **1990**, *112*(23), 8251-8260.
- [57]. Casida, M. E.; Jamorski, C.; Casida, K. C.; Salahub, D. R. *J. Chem. Phys.* **1998**, *108*(11), 4439-4449.
- [58]. Stratmann, R. E.; Scuseria, G. E.; Frisch, M. J. *J. Chem. Phys.* **1998**, *109*(19), 8218-8224.
- [59]. Cancas, E.; Mennucci, B.; Tomasi, J. *J. Chem. Phys.* **1997**, *107*(8), 3032-3041.
- [60]. Harvey, M. A.; Baggio, S.; Garland, M. T.; Baggio, R. *Acta Crystallogr. C* **2008**, *64*(9), 0489-0492.
- [61]. Hensen, K.; Spangenberg, B.; Bolte, M. *Acta Crystallogr. C* **2000**, *56*(2), 208-210.
- [62]. Muthulakshmi, S.; Kalaivani, D. *Acta Crystallogr. E* **2015**, *71*(7), 783-785.
- [63]. Macrae, C.; Bruno, I.; Chisholm, J.; Edgington, P.; McCabe, P.; Pidcock, E.; Rodriguez-Monge, L.; Taylor, R.; van de Streek, J.; Wood, P. *J. Appl. Crystallogr.* **2008**, *41*, 466-470.
- [64]. Bernstein, J.; Davis, R. E.; Shimoni, L.; Chang, N. L. *Angew. Chem. Int. Ed. Engl.* **1995**, *34*(15), 1555-1573.
- [65]. Tanak, H.; Agar, A.; Yavuz, M. *J. Mol. Model.* **2010**, *16*(3), 577-587.
- [66]. Assefa, Z.; Gore, S. B. *Bull. Chem. Soc. Ethiop.* **2016**, *30*(2), 231-239.
- [67]. Günzler, H.; Gremlich, H. U. IR spectroscopy. An introduction. Wiley VCH: Weinheim, 2002.
- [68]. Cruz, C.; Delgado, R.; Drew, M. G.; Felix, V. *J. Org. Chem.* **2007**, *72*(11), 4023-4034.
- [69]. Park, C.; Simmons, H. *J. Am. Chem. Soc.* **1968**, *90*(9), 2431-2432.
- [70]. Koparir, P.; Sarac, K.; Orek, C.; Koparir, M. *J. Mol. Struct.* **2016**, *1123*, 407-415.
- [71]. Pina, J.; Melo, J.; Pina, F.; Lodeiro, C.; Lima, J.; Parola, A. J.; Soriano, C.; Paz Clares, M.; Albelda, M. T.; Aucejo, R. , *Inorg. Chem.* **2005**, *44*, 7449-7458.
- [72]. Jayabharathi, J.; Thanikachalam, V.; Perumal, M. V. *Spectrochim. Acta A* **2012**, *95*, 614-621.
- [73]. O'Boyle, N. M.; Tenderholt, A. L.; Langner, K. M. *J. Comput. Chem.* **2008**, *29*(5), 839-845.
- [74]. Callister, W. D.; Rethwisch, D. G. Materials science and engineering: an introduction. John Wiley & Sons New York: 2007; Vol. 7.
- [75]. Issa, T. B.; Sayari, F.; Ghalla, H.; Benhamada, L. *J. Mol. Struct.* **2018**, *1178*, 436-449.



Copyright © 2019 by Authors. This work is published and licensed by Atlanta Publishing House LLC, Atlanta, GA, USA. The full terms of this license are available at <http://www.eurjchem.com/index.php/eurjchem/pages/view/terms> and incorporate the Creative Commons Attribution-Non Commercial (CC BY NC) (International, v4.0) License (<http://creativecommons.org/licenses/by-nc/4.0>). By accessing the work, you hereby accept the Terms. This is an open access article distributed under the terms and conditions of the CC BY NC License, which permits unrestricted non-commercial use, distribution, and reproduction in any medium, provided the original work is properly cited without any further permission from Atlanta Publishing House LLC (European Journal of Chemistry). No use, distribution or reproduction is permitted which does not comply with these terms. Permissions for commercial use of this work beyond the scope of the License (<http://www.eurjchem.com/index.php/eurjchem/pages/view/terms>) are administered by Atlanta Publishing House LLC (European Journal of Chemistry).